Available online at www.sciencedirect.com

SciVerse ScienceDirect

Geochimica et Cosmochimica Acta 107 (2013) 205–219

Geochimica et Cosmochimica Acta

www.elsevier.com/locate/gca

Non-canonical mass laws in equilibrium isotopic fractionations: Evidence from the vapor pressure isotope effect of SF_6

John Eiler [a,*], Pierre Cartigny [b], Amy E. Hofmann [a], Alison Piasecki [a]

[a] Division of Geological and Planetary Sciences, California Institute of Technology, Pasadena, CA 91125, USA
[b] Laboratoire de Géochimie des Isotopes Stables, Institut de Physique du Globe de Paris, CNRS (UMR 7154), Université Paris Diderot, PRES Sorbonne Paris Cité, 1 rue Jussieu, 75238 Paris Cedex O5, France

Received 21 June 2011; accepted in revised form 29 December 2012; available online 12 January 2013

Abstract

We report experimental observations of the vapor pressure isotope effect, including $^{33}S/^{32}S$ and $^{34}S/^{32}S$ ratios, for SF_6 ice between 137 and 173 K. The temporal evolution of observed fractionations, mass-balance of reactants and products, and reversal of the fractionation at one temperature (155 K) are consistent with a subset of our experiments having reached or closely approached thermodynamic equilibrium. That equilibrium involves a reversed vapor pressure isotope effect; i.e., vapor is between 2‰ and 3‰ higher in $^{34}S/^{32}S$ than co-existing ice, with the difference increasing with decreasing temperature. At the explored temperatures, the apparent equilibrium fractionation of $^{33}S/^{32}S$ ratios is 0.551 ± 0.010 times that for $^{34}S/^{32}S$ ratios—higher than the canonical ratio expected for mass dependent thermodynamic fractionations (~0.515). Two experiments examining exchange between adsorbed and vapor SF_6 suggest the sorbate–vapor fractionation at 180–188 K is similar to that for ice–vapor at ~150 K. In contrast, the liquid–vapor fractionation at 228–300 K is negligibly small (~0.1‰ for $^{34}S/^{32}S$; the mass law is ill defined due to the low amplitude of fractionation). We hypothesize that the observed vapor pressure isotope for SF_6 ice and sorbate is controlled by commonly understood effects of isotopic substitution on vibrational energies of molecules, but leads to both an exotic mass law and reversed fractionation due to the competition between isotope effects on intramolecular vibrations, which promote heavy isotope enrichment in vapor, and isotope effects on intermolecular (lattice) vibrations, which promote heavy isotope enrichment in ice. This explanation implies that a variety of naturally important compounds having diverse modes of vibration (i.e., varying greatly in frequency and particularly, reduced mass) could potentially exhibit similarly non-canonical mass laws for S and O isotope fractionations. We examined this hypothesis using a density function model of SF_6 vapor and lattice dynamic model of $SF_{6(ice)}$. These models support the direction of the measured vapor pressure isotope effect, but do not quantitatively agree with the magnitude of the fractionation and poorly match the phonon spectrum of SF_6 ice. A strict test of our hypothesis must await a more sophisticated model of the isotopic dependence of the phonon spectrum of SF_6 ice.

1. INTRODUCTION

Most terrestrial materials exhibit well-defined relationships between fractionations of two or more independent isotope ratios of a given element (e.g., the $^{17}O/^{16}O$ and $^{18}O/^{16}O$ ratios of oxygen, or the $^{33}S/^{32}S$, $^{34}S/^{32}S$, and $^{36}S/^{32}S$ ratios of sulfur; Hulston and Thode, 1965; Robert et al., 1992). These relationships generally resemble those predicted for equilibrium vibrational isotope effects, which follow a relatively simple, exponential functional form. For example, the following equation describes the expected relationships among fractionations of the sulfur isotopes, ^{32}S, ^{33}S and ^{34}S:

$$\alpha_{33} = \alpha_{34}^{\lambda_{33/34}} \quad (1)$$

* Corresponding author.
E-mail address: eiler@gps.caltech.edu (J. Eiler).

0016-7037/$ - see front matter © 2013 Published by Elsevier Ltd.
http://dx.doi.org/10.1016/j.gca.2012.12.048

where α_{33} and α_{34} values are the $^{33}S/^{32}S$ and $^{34}S/^{32}S$ fractionation factors (e.g., the $^{33}S/^{32}S$ ratio of one material divided by that of another) and $\lambda_{33/34}$ is a constant describing the functional dependence of the fractionation on isotopic mass.

The term 'mass dependent fractionation' is commonly used to describe fractionations that follow a functional form similar to Eq. (1), and where the exponent, λ, exhibits a relatively simple relationship to isotopic mass, predictable from principles of statistical thermodynamics or, for diffusive or gravitational fractionations, the kinetic theory of gases (e.g., Bigeleisen and Mayer, 1947; Hulston and Thode, 1965; Robert et al., 1992; Farquhar and Wing, 2003; Otake et al., 2008; Luz et al., 2009). For example, for equilibrium fractionations of ^{32}S, ^{33}S and ^{34}S in the high-temperature limit, the value of $\lambda_{33/34} = (1/31.97–1/32.97)/(1/31.97–1/33.97) \sim 0.5159$. Similarly, diffusive fractionations of sulfur isotopes associated with Knudsen diffusion of SO_2 gas (i.e., $^{32}S^{16}O_2$, $^{33}S^{16}O_2$ and $^{34}S^{16}O_2$) are expected to follow a fractionation law where $\lambda_{33/34} = \ln(64.96/63.96)^{0.5}/\ln(65.96/63.96)^{0.5} \sim 0.5046$; i.e., the size of the fractionation is a relatively simple function of the mass differences among the isotopic variants of the diffusing gas molecules (Gibbs, 1928). Similar expressions describe the predicted mass laws of many irreversible chemical reactions (Bigeleisen and Wolfsberg, 1958; Young et al., 2002), except some photochemical and related gas phase reactions (Weston, 2006, and references therein); similar mass laws are also expected for gravitational separation (Gibbs, 1928; Grachev and Severinghaus, 2003).

Isotopic fractionations that violate one of these nominally mass-dependent fractionation laws are generally referred to as mass-independent. The strictest definition of mass-independent fractionations is that they involve fractionations of two or more isotope ratios that show no relationship between the magnitude of fractionation and isotopic mass difference; for example, the oxygen isotope fractionation during ozone formation is characterized by $\lambda_{17/18} = 1$ (Thiemens and Heidenreich, 1983). This nomenclature is misleading when applied to mass-dependent fractionations that happen to have mass exponents that differ from common expectations. Here we will use the term 'non-canonical' to refer to mass laws that arise from mass-dependent chemical physics but differ from commonly assumed mass-dependent laws.

Several mechanisms for generating non-canonical mass laws are recognized, most of which involve photochemical reactions and/or nuclear effects restricted to radical species or very high-mass nuclides (Turro, 1983; Bigeleisen, 1996; Clayton, 2002; Weston, 2006; Oduro, 2011); none of these mechanisms should apply to isotopes of low- and moderate-mass elements (H, C, O, S, etc.) undergoing condensed-phase reactions in which no participating species is a radical. An exception to this expectation is a recent theoretical model (Lasaga et al., 2008), which argues that in systems containing weak bonds (e.g., sorption) at relatively high temperature (~300 °C), isotope effects on bond vibration energy can lead to fractionations that differ markedly in mass law from canonical predictions for isotope exchange equilibria. This hypothesis was critiqued in a subsequent paper (Balan et al., 2009), which suggested the Lasaga et al. hypothesis was based on a truncation error in the mathematics used to describe equilibrium fractionations.

Though there is an extensive literature documenting the empirical behaviors of mass exponents describing differences in O and S isotope compositions of natural materials or complex experiments (e.g., Oduro et al., 2011), there remain relatively few studies that examine whether specific equilibrium fractionations follow their expected simple mass-dependent laws (perhaps the best studied case is the water vapor pressure isotope effect; Van Hook, 1968; Luz et al., 2009). Moreover, several recent observations suggest that condensed-phase chemical reactions can lead to non-canonical mass laws for fractionations of O and S isotopes: CO_2 and metal oxides (e.g., CaO, MgO) produced by calcining carbonate minerals (e.g., calcite, dolomite; Miller et al., 2002) exhibit systematic non-canonical, possibly even mass-independent, oxygen isotope fractionations with respect to each other. Similarly, Watanabe et al. (2009) and Oduro et al. (2011) present isotopic analyses of reduced sulfur evolved by heating mixtures of sulfate salts, amino acids, and water. The products of these experiments exhibit non-canonical mass laws for S isotope fractionations with respect to their starting materials. However, in both of these studies, the examined reactions likely involved more than one step, making it challenging to isolate the mass law of any one fractionating process (Oduro et al., 2011). It is not clear whether either of these experiments demonstrates a novel fractionation mechanism that violates common expectations of mass-dependent isotopic fractionation.

We present the results of a set of experiments designed to test the hypothesis that thermodynamically controlled isotope exchange equilibria can lead to non-canonical mass laws for S isotope fractionations. We focus our attention on the vapor pressure isotope effect for various condensed forms of SF_6 (principally ice, but also including several experiments on liquid and adsorbed SF_6). This system was chosen for several reasons: SF_6 is an analyte for the most precise method of sulfur isotope analysis (gas source isotope ratio mass spectrometry), and therefore we can analyze the products of our experiments without the potentially confounding problem of fractionations associated with chemical processing of analytes; the vapor pressure isotope effect has been studied extensively, and so our experimental design and interpretation of results can be placed in the well-established context of past work (Jansco and Van Hook, 1974 and references therein). Finally, SF_6 is a non-polar, symmetric molecule in which only a single isotopic substitution is possible (in the S position; i.e., because F is monoisotopic), and that substitution occurs in the center of the molecule. Similar systems, such as $^{13}C/^{12}C$ fractionations for CH_4, CCl_4 and CO_2 or $^{11}B/^{10}B$ fractionations for BF_3, are known to exhibit reversed vapor-pressure isotope effects (i.e., high-mass isotopologues have higher vapor pressures than low-mass isotopologues) because of the interplay between isotope effects on intermolecular and intramolecular vibrational and rotational energies (Grootes et al., 1969; Jansco and Van Hook, 1974; Eiler et al., 2000). Similar interplay between inter- and intra-molecular

energetics may play a role in creating non-canonical mass laws for vapor pressure isotope effects for the H:D:T and ^{12}C:^{13}C:^{14}C systems (Kotaka et al., 1992; see Section 4). Thus, there are reasons to suspect that SF_6 is a candidate for exhibiting vapor pressure isotope fractionations with a non-canonical mass law.

2. METHODS

The experimental methods and equipment employed in this study are adapted from previous vapor pressure isotope effect studies of CO_2 (Eiler et al., 2000; Rahn and Eiler, 2001). The general goals of our methodology are to determine the equilibrium (i.e., thermodynamically controlled) fractionation between vapor and a condensed phase by demonstrating that the measured fractionation is both time-independent and bracketed (i.e., the same equilibrium state can be reached or closely approached from two or more different initial states), and that this condition can be achieved in a system that conforms to isotopic mass balance (i.e., there are no unaccounted isotopic reservoirs in the experiment). Experimentally measured fractionations that meet these criteria can be relatively confidently interpreted as equilibrium phenomena (Chacko et al., 2001).

Fig. 1 schematically illustrates the vacuum apparatus used for the experiments reported here. All components other than the variable-temperature cryostat and the liquid reservoir are made of Pyrex glass with Teflon Young's valves. The variable-temperature trap was purchased from APD Cryogenics (Model DE-204). The liquid reservoir is constructed of 37 mm OD, 1 mm-walled stainless steel tubing, 55 mm long, that is connected to the rest of the vacuum line via a 120 cm long, 12 mm OD, 1 mm thick tubing (and can be isolated from the rest of the vacuum line through a stainless steel bellows valve). The reservoir in which adsorbed SF_6 is condensed is a glass tube filled with 0.1 μm alumina powder to act as a high-surface area sorption substrate. Pressures within the glass portion of the vacuum line were measured with a Baratron gauge (calibrated with est. 0.1 mbar accuracy based on the previously measured vapor pressure curve of SF_6 ice; Hurly et al., 2000) and, at lower precision, two Thermistor vacuum gauges. The system was evacuated with an oil diffusion pump backed with a 2-stage rotary pump and achieved baseline pressures of $\sim 10^{-6}$ mbar.

Four different kinds of experiments were conducted:

(1) *Procedural blanks:* Gas was expanded into the variable-temperature trap at temperatures and pressures that should not lead to condensation of SF_6 (either 300 K and 62 mbar or 220 K and 26 mbar). After 30 min, a valve was closed to isolate the vapor inside the trap volume from vapor outside that trap, and the two aliquots were recovered from the vacuum line and analyzed for their isotopic composition. These experiments were conducted to examine whether vapor could be moved and stored throughout the vacuum apparatus—with and without temperature gradients (e.g., Sun and Bao, 2011a,b)—without fractionation when no condensed form of SF_6 was present.

(2) *Diffusion:* Gas was expanded into a portion of the vacuum apparatus and then gradually admitted into another, previously evacuated, portion by opening a valve just enough to permit slow leakage across the seal. The valve was then tightly shut when a large

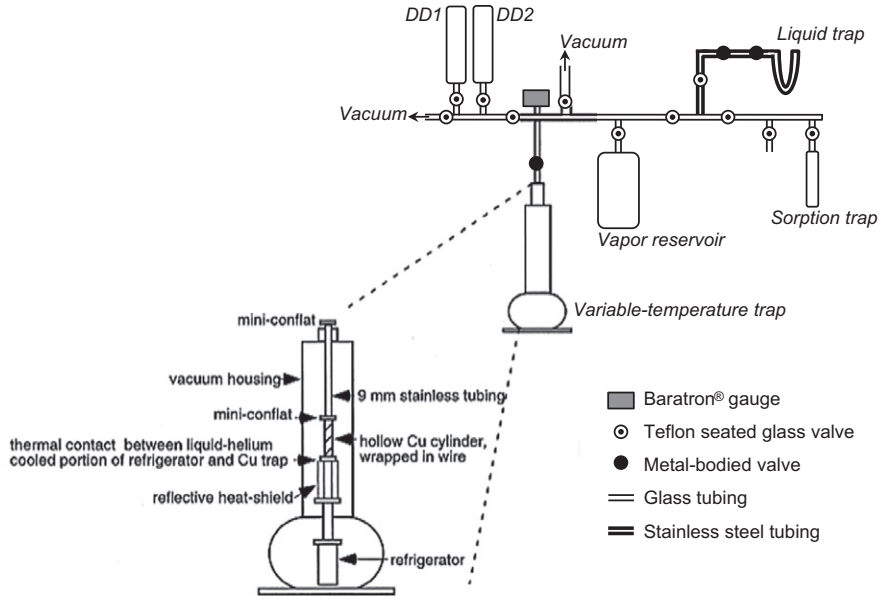

Fig. 1. Schematic illustration of the vacuum apparatus used to conduct the experiments described in this study. Volumes defined by light lines are glass walled; heavy lines indicate metal walled tubing. 'DD1' and 'DD2' indicate the volumes containing the starting gases for all experiments. The inset shows the interior components of the liquid-He-cooled variable temperature trap (all metal construction) used for all ice–vapor experiments.

pressure imbalance still remained across the valve. This experiment created an opportunity for diffusive fractionation, and it therefore permitted us to observe the amplitude and mass law of such fractionations.

(3) *Synthesis:* An aliquot of vapor was exposed to the variable-temperature trap (for ice), chilled stainless steel trap (for liquid), or chilled reservoir of sorption substrate (for sorbate) at pressures significantly above saturation with respect to ice, liquid, or sorbed SF_6, respectively, leading to growth of a condensed phase of SF_6. Pressure generally stabilized within a few seconds (up to several minutes for sorbate experiments). Vapor was left in contact with the condensed phase for a defined period of time, varying from a few seconds to several days, after which the trap containing the condensed phase was isolated by closing a valve. The trap was warmed to fully vaporize the trapped condensate, and the two fractions (vapor and condensate) were collected separately for isotopic analysis. The SF_6 recovered from the condensate trap always contained a small amount (up to a few per cent, relative) of SF_6 vapor that was in the interior volume of the trap when it was isolated; therefore, isotopic compositions of condensates are calculated by making a small correction to their measured composition to remove contributions from co-collected vapor. This calculation is based on the known volume of the trap and the known pressure and isotopic composition of vapor at the end of the experiment (which is recovered without contamination by condensate in the vapor fraction). This correction is too small and well-constrained to lead to a significant artifact in the mass law we estimate for equilibrium vapor pressure isotope effects (below).

(4) *Reversal:* Reversal experiments generally follow the methods of synthesis experiments but with the following changes: First, experiments #20–22 followed condensation protocols different from synthesis experiments: in experiments #20–21 the gas was exposed to the trap at room temperature and then the trap was gradually (over tens of minutes) cooled to 155 K; in experiment 22 gas was quantitatively condensed in the trap at 100 K and then trap was gradually warmed (again, over tens of minutes) to 173 K to establish a stable vapor pressure. This was done in an effort to promote growth of high-surface-area ice. In all cases, after the condensate (always ice) had grown and the vapor pressure stabilized, the trap containing the condensate was isolated from vapor by closing a valve. The vapor reservoir was then fully evacuated and re-filled with SF_6 vapor of a markedly different isotopic composition, to very nearly the same pressure (generally within a few %, relative) as the stable equilibrium pressure. The valve separating the new vapor from the previously grown condensate reservoir was then opened, allowing isotopic exchange between the two phases. The experiment then proceeded as for a synthesis experiment. We could not precisely evaluate mass balance for these experiments because the two reservoirs of SF_6 differed greatly in isotopic composition and mixing proportions of old and new vapor were not sufficiently well controlled. Therefore, our evaluations of mass balance focus on synthesis experiments, where the system remains nominally closed throughout the experiment.

Most experiments conducted over the course of this study were ice synthesis experiments or reversal experiments in which the condensed phase was SF_6 ice. A subset of ice synthesis and reversal experiments were conducted with the cold trap filled with silica sand in another attempt to promote growth of high-surface-area ice. These experiments occurred in the solid SF_6 stability field and the fast rate of condensation differed markedly from adsorption experiments; we conclude that ice, rather than adsorbed SF_6, was grown on the silica sand in these experiments.

All starting gases and experimental run products were analyzed in the IPGP laboratory for stable isotope geochemistry (Paris) by dual inlet gas source isotope ratio mass spectrometry using a Thermo irms-253. All gases used in the present study were high purity grade (i.e., nominally >99.999% pure). In particular, we found no evidence that our in-house reference gas contained impurities such as C_3F_6, a fragment of which can yield an isobaric interference at $m/z = 131$. The $^{33}S/^{32}S$, $^{34}S/^{32}S$ and $^{36}S/^{32}S$ isotope ratios are directly calculated from the ion currents at $m/z = 127$, 128, 129, 131. Measurements of IAEA-S1 over two years in this laboratory give $\Delta^{33}S$ and $\Delta^{36}S$ of 0.081 ± 0.005 and -0.62 ± 0.11, respectively; these values are within the error of the values observed in the sulfur isotope laboratory at the University of Maryland (see Table 2 in Ono et al., 2006). Each measurement included determination of the $\delta^{33}S$, $\delta^{34}S$, and $\delta^{36}S$ values. Though the $\delta^{36}S$ values we observed are generally correlated with concurrent $\delta^{33}S$ and $\delta^{34}S$ measurements, a subtle but, for our purposes, significant ($\sim$0.1‰ to 1.0‰) scatter of $\delta^{36}S$ results suggests either influence of an isobaric interference in some measurements of this relatively low abundance isotope ($\sim$0.02% of natural sulfur) or uncontrolled analytical artifacts. The former is supported by the fact that a plot of $\delta^{36}S$ vs. $\delta^{34}S$ for all ice synthesis experiments yields an intercept substantially different from zero (-0.81 ± 0.01‰, 1σ; this is consistent with loss of a ^{36}S isobar during ice growth, perhaps because it is cryogenically removed). Therefore, all $\delta^{36}S$ values collected over the course of this study are presented in the Supplemental information, and only $\delta^{33}S$ and $\delta^{34}S$ values are reported in the main body of this paper.

All sulfur isotope ratios are reported relative to the Vienna Canyon Diablo Meteorite standard. The working gas used as an intralaboratory standard for all mass spectrometric measurements reported here has a nominal composition of $\delta^{33}S_{VCDT} = 8.714$‰ and $\delta^{34}S_{VCDT} = 16.990$‰ (calibrated by comparison with the IAEA-S-1 interlaboratory sulfur isotope standard). This is closely similar to the products of most experiments (e.g., 'raw' $\delta^{33}S$ values of most gases, measured vs. the working gas, are $\sim$1‰). This compositional similarity of unknowns and intralaboratory standards reduces the risk that our results are influenced

by unrecognized non-linearities in mass spectrometric results. Standard errors for individual mass spectrometric measurements averaged ±0.005‰ for $\delta^{33}S$, ±0.003‰ for $\delta^{34}S$ (1 standard error). Replicate analyses of the same gas generally reproduce with a standard deviation of 1–2 times these standard errors. All experiments were performed with one or both of two synthetic SF_6 gases: 'DD-1' ($\delta^{33}S_{VCDT} = 8.512‰$, $\delta^{34}S_{VCDT} = 16.583‰$) and 'DD-2' ($\delta^{33}S_{CDT} = 0.875‰$, $\delta^{34}S_{CDT} = 1.648‰$).

The stable isotope laboratory at the IPG-Paris has examined a wide range of natural samples and interlaboratory standards to establish the accuracy with which our mass spectrometric measurements reproduce the mass laws expected for common natural fractionation processes (i.e., the 'terrestrial mass fractionation line'). These measurements yielded a slope of 0.51593 in a plot of $\delta^{33}S^*$ vs. $\delta^{34}S^*$ (where $\delta^x S^* = 10^3 \ln\delta^x S/1000 + 1$), see Hulston and Thode, 1965; Miller et al., 2002). This slope compares with the canonical value of 0.515 commonly used to interpret sulfur isotope measurements of terrestrial materials (though predicted mass exponents for equilibrium fractionations are expected to vary by up to ~1–2%, relative, about this value, depending on temperature and the reduced mass and frequencies of relevant bond vibrations; e.g., Otake et al., (2008).

3. RESULTS

Table 1 reports the isotopic compositions of all experimental run products analyzed in this study. Where a condensate fraction was collected with a small proportion of vapor from the trap headspace, the composition reported in Table 1 reflects the corrected composition of condensate alone (i.e., after removing the contribution from co-collected vapor). The correction is smaller than 0.4‰ in $\delta^{34}S$ in all cases and was negligible (<<0.1‰) for experiments #16, 17, 19 and 20 (note that experiment 20 is particularly significant because it demonstrates that our protocol can achieve a reversible equilibrium). The mass exponent ($\lambda_{33/34}$) calculated for each experiment is insensitive to this mass-balance correction (i.e., increasing or decreasing the size of this correction slightly changes the amplitude of inferred fractionations without significantly changing the inferred mass law of that fractionation).

In one experiment (#11 in Table 1), the total amount of SF_6 recovered from both the vapor and ice reservoirs was only 84% of the initial amount at the start of the experiment. A gas handling error is implied, possibly an unrecognized slow leak that gradually evacuated part of the sample, or a stuck valve that prevented recovery of vapor from a portion of the vacuum line. In any event we report the results of this experiment but distinguish it with a gray font in Table 1 and do not include it in any of our figures or consider it in any of our interpretations.

Vapor from one procedural blank experiment (63 mbar of SF_6 vapor exposed to the cold trap held at 300 K; Experiment 1 in Table 1) was recovered as a single aliquot (i.e., combining vapor inside and outside the trap) and yielded an isotopic composition within the range of compositions measured for aliquots of the DD-1 gas reservoir. This experiment simply demonstrates that there are no fractionating additions or losses of SF_6 (or contaminants that lead to isobaric interferences) that result from exposure to various parts of the vacuum line. Vapor from a second experiment of this type (26 mbar pressure and a trap held at 220 K; Experiment 2 in Table 1) was recovered as two separate aliquots ('trap' and 'vapor'). These two aliquots exhibit a relatively small fractionation with respect to each other (<0.1‰ in both $\delta^{33}S$ and $\delta^{34}S$) and their weighted average is comparable to the initial value of the DD-1 gas reservoir used for the experiment. It is imaginable that this experiment exhibits a subtle fractionation due to the 80 K temperature gradient between the trap and the rest of the vacuum apparatus. We examine this possibility further when the mass laws of synthesis fractionations are discussed, below. In any event, we conclude that gases can be exposed to various components of our apparatus, including a chilled (but ice-undersaturated) trap, with fractionations in $\delta^{33}S$ and $\delta^{34}S$ that are small multiples of analytical precision (and, it will be shown, much smaller than fractionations resulting from exposure to condensed SF_6).

The diffusion experiment conducted at room temperature (Experiment 3 in Table 1) yielded similarly negligible (<0.05‰) differences between diffused and residual gas for both $\delta^{33}S$ and $\delta^{34}S$ and a weighted average within the range of aliquots of the starting gas. While this fractionation is too small to yield a meaningful estimate of the exponent that characterizes the mass law for diffusive fractionation (i.e., its $\lambda_{33/34}$ value), this result demonstrates that it is unlikely we generated significant isotopic fractionations through accidental diffusive losses of gas; i.e., this experiment re-enforces our conclusion that gases can be transferred through our apparatus with negligible fractionations provided no condensed phase of SF_6 is formed.

Synthesis experiments (Experiments 4 through 17 in Table 1) in which ice was grown exhibit a systematic dependence of the amplitude of the ice–vapor S isotope fractionation on both the duration of the experiment and the ice/vapor ratio (Figs. 2 and 3). Experiment 4, which lasted 10 s (i.e., the vapor and condensate were isolated from one another immediately after pressure stabilized) exhibits negligible (<0.05‰) ice–vapor fractionations for $\delta^{33}S$ and $\delta^{34}S$, indicating that the process of ice growth from vapor involves no significant fractionations. For all experiments in which ice was substantially more abundant than vapor (by a factor of ~5 or more), the ice–vapor fractionation increased monotonically over a period of ~ 1 h, and then remained nearly constant for all longer durations examined in our experiments (out to 90 h; Fig. 2). For all experiments lasting 1 h or longer (i.e., long enough to have reached the time-invariant period in Fig. 2), there is an increase in the measured fractionation with increasing proportion of ice (Fig. 3). We have evaluated the isotopic mass balance of all synthesis experiments by calculating the weighted average composition of the vapor and condensate fractions of each experiment (Table 1). These weighted averages—$\delta^{33}S_{VCDT} = 8.536 \pm 0.018$, $\delta^{34}S_{VCDT} = 16.635 \pm 0.035$—vary little from one experiment to another and are comparable to the starting composition of the DD-1 gas

Table 1
Experimental results.

Experiment number	Experiment type	Condensed phase	Temperature (K)	Duration (min)	Fraction condensate	$\delta^{33}S_{CDT}$ vapor	$\delta^{34}S_{CDT}$ vapor	$\delta^{33}S_{CDT}$ condensate	$\delta^{34}S_{CDT}$ condensate	$\delta^{33}S_{CDT}$ bulk	$\delta^{34}S_{CDT}$ bulk	$1000\cdot\ln(\alpha_{33})$ cond-vap	$1000\cdot\ln(\alpha_{34})$ cond-vap	$\lambda_{33/34}$ cond-vap	Fractional equilibration[##]
1	Procedural blank	None	300	30	–	8.501	16.572	–	–	8.501	16.572	–	–	–	
2	Procedural blank	None	220	30	–	8.586	16.714	8.517[*]	16.633[*]	8.559	16.683	−0.068	−0.080	0.850[&]	
3	Diffusion	None	300	3	–	8.516[@]	16.621[@]	8.550[#]	16.671[#]	8.538	16.654	0.033	0.049	0.673[&]	
4	Synthesis	Ice	150	0.17	0.865	8.568	16.705	8.545	16.662	8.548	16.668	−0.022	−0.043	0.525[&]	
5	Synthesis	Ice	155	38	0.859	9.030	17.511	8.441	16.432	8.524	16.585	−0.584	−1.061	0.550	
6	Synthesis	Ice	155	60	0.562	8.894	17.272	8.283	16.137	8.551	16.634	−0.605	−1.116	0.542	
7	Synthesis	Ice	160	60	0.647	9.007	17.476	8.244	16.127	8.514	16.603	−0.756	−1.327	0.569	
8	Synthesis	Ice	141	60	0.742	9.112	17.683	8.354	16.320	8.549	16.672	−0.751	−1.339	0.561	
9	Synthesis	Ice	150	80	0.864	9.727	18.778	8.329	16.276	8.519	16.616	−1.385	−2.459	0.563	
10	Synthesis	Ice	155	1200	0.872	9.606	18.574	8.394	16.390	8.550	16.670	−1.201	−2.147	0.559	
11[$]	Synthesis	Ice	155	2520	0.851	9.654	18.690	8.366	16.352	8.558	16.700	−1.276	−2.298	0.555	
12	Synthesis	Ice	155	5340	0.871	9.798	19.004	8.433	16.471	8.609	16.798	−1.353	−2.488	0.544	
13	Synthesis	Ice	155	2880	0.870	9.658	18.657	8.400	16.402	8.564	16.696	−1.247	−2.216	0.563	
14	Synthesis	Ice	155	5400	0.861	9.582	18.522	8.401	16.394	8.565	16.689	−1.170	−2.091	0.560	
15	Synthesis	Ice	155	1440	0.857	9.629	18.612	8.426	16.429	8.598	16.741	−1.192	−2.145	0.556	
16	Synthesis (SiO_2)	Ice	155	3960	0.969	9.741	18.857	8.545	16.628	8.583	16.697	−1.185	−2.190	0.541	
17	Synthesis (SiO_2)	Ice	137	5310	0.996	10.198	19.678	8.525	16.609	8.532	16.621	−1.657	−3.014	0.550	
18	Reversal	Ice	155	3720	0.857	6.953	13.446	7.799	15.242	–	–	0.840[**]	1.770[**]	0.474[**]	0.749
19	Reversal	Ice	155	8682	0.994	8.715	16.870	8.500	16.541	–	–	−0.213[**]	−0.323[**]	0.659[**]	0.890
20	Reversal	Ice	155	6780	0.997	9.976	19.268	8.675	16.890	–	–	−1.289	−2.336	0.552	1.008
21	Reversal (SiO_2)	Ice	155	8580	0.997	8.793	17.012	8.550	16.679	–	–	−0.241[**]	−0.328[**]	0.735[**]	0.891
22	Reversal (SiO_2)	Ice	173	11100	0.976	7.505	14.473	8.469	16.519	–	–	0.957[**]	2.015[**]	0.475[**]	–
23	Synthesis	Adsorbate	179.5	21	0.883	9.385	18.257	8.338	16.271	8.460	16.503	−1.038	−1.952	0.532	
24	Synthesis	Adsorbate	188	60	0.812	9.095	17.644	7.967	15.626	8.179	16.005	−1.119	−1.985	0.564	
25	Synthesis	Liquid	300	40	0.743	8.586	16.771	8.537	16.654	8.549	16.684	−0.049	−0.115	0.426[&]	
26	Synthesis	Liquid	228	45	0.918	8.443	16.489	8.523	16.605	8.517	16.595	0.080	0.114	0.702[&]	

[*] No condensate present; composition of 'condensate' reflects vapor contained in bare cold trap.
[@] Diffused gas in diffusion experiment.
[#] Residual gas in diffusion experiment.
[$] Recovered vapor and ice fractions at end of experiment less than amount of starting gas.
[&] Amplitude of fractionation too low for confident estimate of $\lambda_{33/34}$.
[##] Fractional approach of an ice reversal experiment to the time-invariant fractionation of ice-rich synthesis experiments at the same temperature.
[**] Note fractionation reflects imperfect equilibration of DD-2 vapor with ice grown from DD-1.

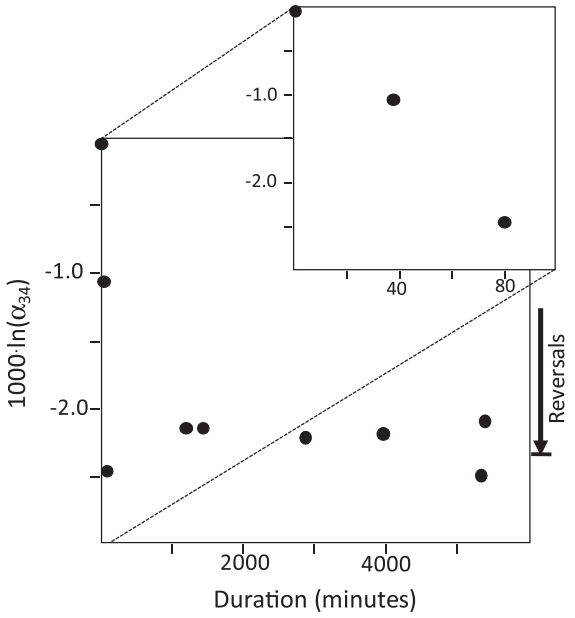

Fig. 2. Ice–vapor sulfur isotope fractionations ($1000 \cdot \ln\alpha_{34}$, where α_{34} is calculated as $R^{34}_{ice}/R^{34}_{vapor}$), for synthesis experiments conducted at 150 or 155 K and having more than 85% of the SF_6 in the system as ice (i.e., 15% or less as vapor), plotted vs. the duration of the experiment. Note that experiments differ in fraction of ice and temperature, both factors that contribute to variations in fractionation at a given time (Figs. 3 and 4). Fractionations are negligible immediately after ice has condensed from vapor, grow to ~2.2‰ over a period of 1 h (see inset), and then remain near this value for up to 90 h. The arrow on the right side of the main panel indicates the direction of approach to the time-independent value of reversal experiments, and the head of the arrow lies at the fractionation reached by Experiment 20 (6780 min duration). Experiment 11, which failed to recover all of the SF_6 introduced to the apparatus at the beginning of the experiment, has been excluded.

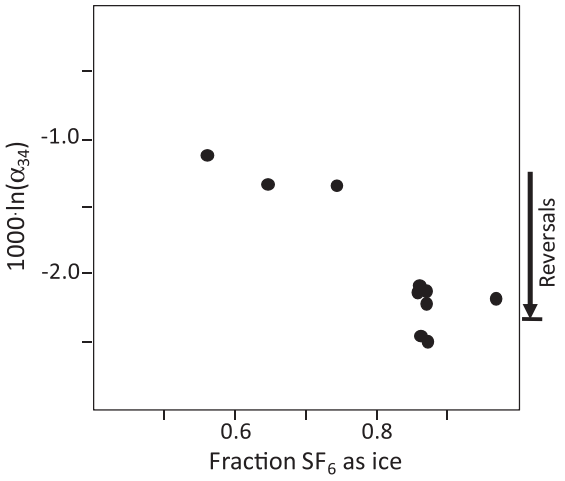

Fig. 3. Ice–vapor sulfur isotope fractionations ($1000 \cdot \ln\alpha_{34}$, where α_{34} is calculated as $R^{34}_{ice}/R^{34}_{vapor}$), for synthesis experiments conducted between 141 and 160 K and lasting 1 h or more, plotted vs. the fraction of SF_6 in the system as ice (i.e., moles of SF_6 ice divided by the sum of moles of SF_6 ice and vapor). Note that experiments differ in temperature, which can contribute to variations in fractionation at a given time (Fig. 4); it is also possible that some of the experiments conducted for 60 min had not quite reached the time-independent fractionation (Fig. 2). Fractionations increase with increasing fraction of ice, though this dependence is a small proportion of the overall fractionation when the fraction of ice exceeds ~85%. The arrow on the right side of this figure indicates the direction from which reversal experiments at 155 K approached this time-independent value, with the head of the arrow sitting at the ice content and fractionation reached by Experiment 20 (99.7% ice). Experiment 11, which failed to recover all of the SF_6 introduced to the apparatus at the beginning of the experiment, has been excluded.

reservoir that was used for all synthesis experiments. This result suggests that we have accurately corrected the compositions of condensates to account for the small amount of co-collected vapor in the headspace of the trap.

The behaviors we observe for ice synthesis experiments closely resemble results from a previous study of the vapor pressure isotope effect for CO_2 ice (Eiler et al., 2000). We suggest a similar interpretation, i.e., that equilibrium between vapor and the surfaces of ice crystals (extending to some unknown but presumably shallow depth) is rapid—on the time scale of an hour. Because solid state diffusion is generally slow at the temperatures of our experiments, we suggest that the mechanism of this exchange is steady state exchange of vapor with a surface layer of the ice, where no net growth or sublimation of ice is occurring but the residence time of any one molecule in the near-surface of the condensed phase is short (though doubtless a detailed model of the kinetics of such processes would need to consider ice crystal size, porosity, the relative rates of surface exchange and volume diffusion, and perhaps other issues). In this case, the equilibrium ice–vapor fractionation can be attained quickly, but will only be observed at its full magnitude when the amount of exchangeable (presumably near-surface) ice substantially exceeds the amount of vapor. This is because the condensate recovered from the trap at the end of the experiment is a mixture of exchangeable condensate and non-exchangeable condensate (presumably the interiors of ice crystals). If the exchangeable reservoir is relatively small compared to vapor, the exchangeable condensate reservoir will change significantly from its initial composition due to exchange with vapor, but that change will not be observed because of dilution by unexchangeable ice.

It would be difficult to confidently establish what fraction of the ice reservoir is exchangeable based on synthesis experiments alone, and it may vary from experiment to experiment. A reasonable approximation might be made by extrapolating the trend of data for synthesis experiments in Fig. 3 to proportions of ice approaching 1; on this basis, experiments with more than ~85% of the SF_6 as ice would appear to come within ~10%, relative, of the ice-vapor equilibrium. An additional constraint can be found in our attempts to reverse the ice–vapor fractionation through 'reversal experiments' (the fourth protocol described above). If the same ice–vapor fractionation is observed in both a synthesis and reversal experiment conducted under the same conditions, we can be confident that we are

achieving sufficiently ice-rich conditions that the vapor is effectively buffered by the reservoir of exchangeable ice without significantly modifying the composition of that reservoir. Our reversal protocol involves exposing pre-formed ice grown from the DD-1 vapor reservoir to a vapor reservoir composed of DD-2 vapor. The DD-2 reservoir is ~17.5‰ lower in $\delta^{34}S$ than the vapor in equilibrium with the DD-1 reservoir. Thus these experiments present a stringent test of reversal; i.e., we will only observe a fractionation within 0.1‰ of that seen in synthesis experiments if the exchangeable ice is ~200× the size of the vapor reservoir. We can estimate the fractional approach to reversal through the index: $(\Delta^{34}S_{rev} - \Delta^{34}S_{syn})/([\delta^{34}S_{cond} - \delta^{34}S_{DD2}] - \Delta^{34}S_{syn})$, where the $\Delta^{34}S_{rev}$ is the observed ice–vapor fractionation of the reversal experiment, $\Delta^{34}S_{syn}$ is the ice–vapor fractionation of a synthesis experiment done under the same conditions, $\delta^{34}S_{cond}$ is the $\delta^{34}S_{cond}$ value of ice in the reversal experiment, and $\delta^{34}S_{DD2}$ is the composition of the DD2 gas reservoir (see Table 1). By this criterion, experiment 20 fully reverses (100% equilibration) synthesis experiments done at 155 K, experiments 19 and 21 achieved only 89% equilibration, and the relatively ice-poor reversal experiment 18 reached only 75% equilibration. We conclude that, though it is challenging to produce enough exchangeable ice to fully (better than 99%) reverse an experiment, this is possible and has been achieved at 155 K. We cannot make such an estimate for experiment 22 because there is no accompanying synthesis experiment done at exactly the same temperature (173 K).

The failure of experiments 18, 19 and 21 to achieve a full reversal of the 155 K synthesis fractionation presumably reflects the large isotopic contrast between the DD-1 and DD-2 reservoirs and the low fraction of ice that is exchangeable. Nevertheless, it is clear that synthesis experiments in which 85% or more of the SF_6 is ice also closely approximate the reversible fractionation achieved in Experiment 20 (Fig. 3). We suggest that these synthesis experiments also usefully constrain the equilibrium fractionation (though some of these could under-estimate the magnitude of that fractionation because of differences in composition between exchangeable and non-exchangeable ice). Before including these data in our discussion of equilibrium fractionations, it is important to consider the effect of mixing unexchanged and exchanged ice on the amplitude and mass law of observed fractionations: Consider the case where the true equilibrium ice–vapor fractionation in $^{34}S/^{32}S$ ratio ($1000 \cdot \ln\alpha_{34}$) is exactly 2.2‰ and is characterized by a mass exponent ($\lambda_{33/34}$) of exactly 0.5500 (i.e., like the reversed equilibrium at 155 K seen in experiments 16 and 20). If this equilibrium occurred in a system composed of 85% ice and 15% vapor, and if only 50% of that ice were exchangeable, then the measured ice–vapor fractionation would be 1.913‰ and the measured $\lambda_{33/34}$ would be 0.5500. Given that measured fractionations vary little among experiments containing between 85% and 100% ice, this example likely presents an extreme case. We conclude that if we include synthesis data from experiments having >85% ice, we will slightly under-estimate the amplitude of the ice–vapor fractionation but engender no meaningful error in its mass exponent.

All nominally equilibrated ice–vapor fractionations exhibit inverse vapor pressure isotope effects (i.e., condensate is poorer in heavy isotopes than vapor). All ice synthesis experiments lasting less than 1 h and/or having less than 85% of SF_6 as ice also exhibit inverse vapor pressure isotope effects, albeit lower in amplitude than the nominally equilibrated experiments (presumably because they have only partially approached the final, equilibrated state).

We conducted two sorbate synthesis experiments: one at 180 K and the other at 188 K (Experiments 23 and 24, respectively). These experiments were conducted by slowly (over several minutes) condensing SF_6 onto alumina powder at temperatures well above the freezing point of SF_6, lasted 21 and 60 min, respectively, and were conducted at significantly different proportions of sorbate (i.e., adsorbed SF_6) vs. vapor (Table 1). Despite these differences, the two experiments yielded essentially indistinguishable results. While a fuller exploration of these parameters would be required to be certain, this result suggests that the sorbate reservoir exchanges over a time scale comparable to or faster than the surface of ice (i.e., within an hour or less), and that, unlike ice, sorbate is fully exchangeable. Rahn and Eiler (2001) reached similar conclusions based on a more extensive study of the vapor pressure isotope effect of adsorbed CO_2 under conditions similar to the experiments reported here. The weighted average isotopic compositions of condensate and vapor in both experiments were closely similar to the accepted composition of the DD-1 reservoir of starting vapor. Both experiments yielded a significant inverse vapor pressure isotope effect; i.e., the sorbate–vapor fractionation broadly resembles the equilibrium ice–vapor fractionation (Fig. 4).

The two liquid synthesis experiments (experiments 25, done at 300 K, and 26, done with the liquid reservoir at 228 K) yielded small fractionations of ca. $\leqslant$0.1‰ between liquid and vapor for both α_{33} and α_{34}. The weighted averages of condensate and vapor in both experiments were similar to the composition of the DD-1 reservoir of starting vapor. Taken at face value, these results imply a 'normal' vapor pressure isotope effect (i.e., liquid enriched in heavy isotopes) at 228 K and an inverse isotope effect at 300 K.; however, these fractionations are small multiples of analytical precision and we are not confident that they are well resolved from 0. We did not conduct time-series experiments for liquid synthesis or examine variations in the liquid/vapor ratio. However, given that liquids should be well-mixed by internal diffusion and convection over the time scales of our experiments, and based on our experience with ices and previous studies of liquid vapor pressure isotope effects (Jansco and Van Hook, 1974, and references therein), we suspect that any experiment lasting ~1 h or more should exhibit a liquid–vapor fractionation closely approximating equilibrium.

Fig. 4 summarizes the results of all experiments discussed above, plotted in dimensions of $1000 \cdot \ln(\alpha_{33})$ vs. $1000 \cdot \ln(\alpha_{34})$; for reference, we plot lines corresponding to various values of $\lambda_{33/34}$, where $\alpha_{33} = \alpha_{34}\ ^{\lambda_{33/34}}$. All equilibrated ice synthesis and reversal experiments, all partially equilibrated ice synthesis experiments, and both sorbate synthesis experiments (which we also infer reached or

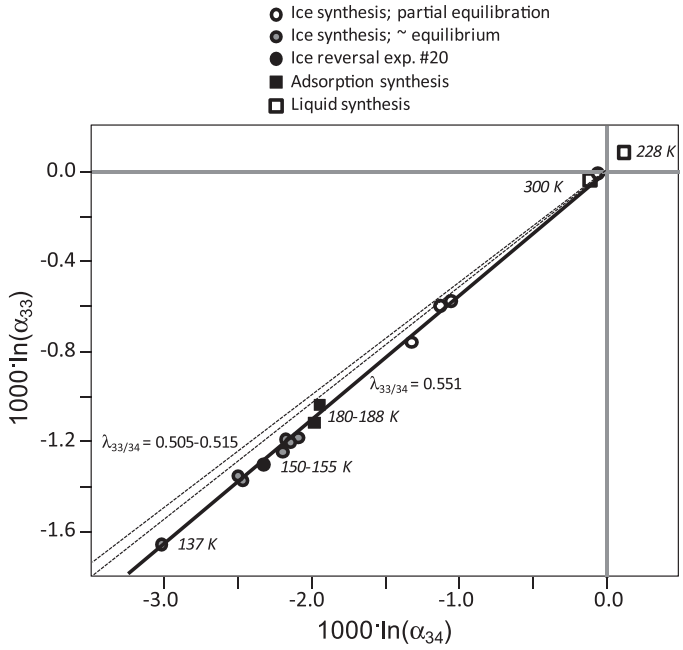

Fig. 4. Comparison of $^{33}S/^{32}S$ ratio fractionations ($1000 \cdot \ln\alpha_{33}$, where α_{33} is calculated as $R^{33}_{condensate}/R^{33}_{vapor}$) to $^{34}S/^{32}S$ ratio fractionations ($1000 \cdot \ln\alpha_{34}$, where α_{34} is calculated as $R^{34}_{condensate}/R^{34}_{vapor}$) for all ice–vapor, sorbate–vapor and liquid–vapor exchange experiments (excepting Experiment 11, which suffered from a significant gas handling error, and the reversal experiments that only achieved partial equilibration). The slope of a line joining an experimental point in this plot to the origin (which lies at the intersection of the two gray lines) corresponds to the $\lambda_{33/34}$ value of the fractionation for that experiment. All data fall along a trend similar to a line of slope 0.551. Lines of slope 0.505–0.515 (the expected range of canonical mass dependent fractionation slopes) are indicated with dashed lines.

closely approached equilibrium) closely conform to a single trend corresponding to a $\lambda_{33/34}$ value 0.551. The result is consistent with a single mechanism of fractionation having a single mass exponent (i.e., there is no evidence that the mass exponent of the fractionation changes as the equilibrium condition is approached or as we change proportions of condensate and vapor). This value is significantly higher than the range of slopes expected for all recognized S isotope fractionations that follow a canonical mass-dependent process (dashed lines in Fig. 4; e.g., Otake et al., 2008). Thus, the vapor pressure isotope effect for SF_6 ice appears to be non-canonical in its mass law, and the limited number of observations of vapor–sorbate systems suggests the same is true of adsorbed SF_6.

4. DISCUSSION

The results we present for ice–vapor exchange experiments meet the criteria commonly used to establish whether an isotope exchange experiment has reached or closely approached thermodynamic equilibrium: the fractionations we observe are time-invariant, reversible (at least at 155 K, where the largest number of our experiments were done), and occur in systems that conform to mass balance (i.e., the weighted average of products equals that of reactants). Therefore, it seems reasonable to interpret these results in light of the chemical physics known to control equilibrium vapor pressure isotope effects. We have not demonstrated reversibility of the sorbate–vapor and liquid–vapor fractionations, but we comment on this more limited set of experiments where they are relevant to our general argument.

4.1. A conceptual model for the non-canonical mass law for the VPIE of SF_6

We propose that the non-canonical character of the mass law for the vapor pressure isotope effect for SF_6 ice and sorbate results from a combination of isotope effects on the vibrational energies of intermolecular bonds between adjacent SF_6 molecules in condensate (i.e., lattice modes in ice) and isotope effects on the vibrational energies of intramolecular S–F bonds within the SF_6 molecule in both vapor and condensate. These two classes of bonds differ in several respects: The intermolecular bonds arise from dipole–dipole coupling, are relatively weak (~1 N/m), and the vibrating species is a relatively large (146 amu), internally rigid molecule (Salvi and Schettino, 1979; Firanescu et al., 2008). The intramolecular vibrations, in contrast, involve stiff covalent bonds (typically force constants of ~ hundreds of N/m; Thornton and Rex, 1993) and the vibrating species (S and F) have relatively low reduced mass.

To illustrate this point, consider the case in which we adopt the expression describing the mass laws of equilibrium fractionations in the high temperature limit ($\lambda = [1m_1 - 1/m_2]/[1/m_1 - 1/m_3]$; Young et al., 2002) and use this expression to calculate separate λ values associated with the intra- and intermolecular vibrations. This treatment is clearly inaccurate in detail both because intra and intermolecular motions are not independent in condensed

phases and because the high temperature limit does not apply to the low temperature conditions of our experiments. Nevertheless, this expression provides a simple basis for illustrating the relationship between reduced mass and mass law. In this case, the isotope effects acting on intermolecular vibrations (i.e., treating each SF_6 group as an internally rigid point mass) will lead to fractionations having $\lambda_{33/34}$ values of ~0.503, whereas $\lambda_{33/34}$ values for isotopic fractionations driven by intramolecular vibrations will be ~0.513—similar to the canonical value often used to describe equilibrium fractionations. A key point is that the mass law of a fractionation that combines both of these effects can take on other values, possibly higher or lower than either, depending on whether inter- and intramolecular vibrational isotope effects drive fractionations of the same or different sign (see schematic illustration in Fig. 5). If these two factors have the same sign (e.g., if both promote concentration of heavy isotopes in condensate relative to vapor), then the $\lambda_{33/34}$ value of the net fractionation will lie between 0.503 and 0.513 (Fig. 5a). However, if these two factors act in opposite directions (e.g., if intermolecular, or lattice, vibrational isotope effects promote concentration of heavy isotopes in the condensate whereas intramolecular vibrational isotope effects promote concentration of heavy isotopes in vapor), then the $\lambda_{33/34}$ value of the resulting net fractionation can take on a wider range of values, depending on the relative magnitudes of these two factors (Fig. 5b). Note we discuss these modes of vibration as if their energies were independent as a simplifying rhetorical device; a quantitative treatment of such problems must consider the fact that the presence of lattice modes influences the intramolecular vibrations and vice versa.

Intermolecular vibrations generally promote concentration of heavy isotopes into condensates because heavy isotopic substitution reduces frequencies of these vibrations, stabilizing the condensate, and there is no competing effect in the vapor (i.e., because vapor lacks stable intermolecular bonds; note that the hindrance of rotational modes in liquids can be an exception to this generalization; Jansco and Van Hook, 1974). In contrast, molecular ices and liquids commonly exhibit decreases in frequencies of intramolecular vibrations relative to vapor (Jansco and Van Hook,

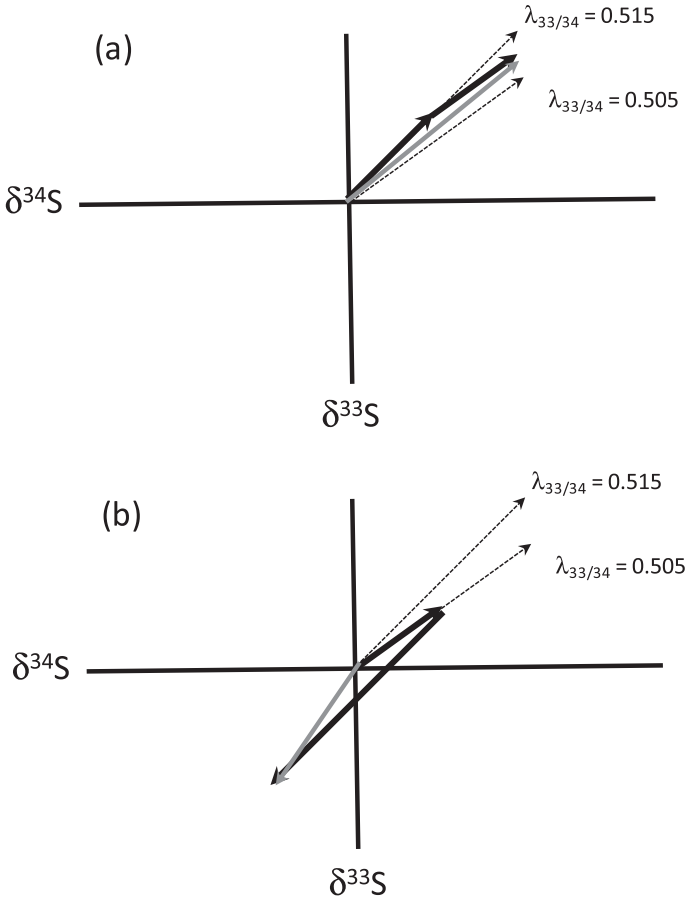

Fig. 5. Illustration of the net fractionations that result from combination of two components that differ significantly in $\lambda_{33/34}$ value. Panel (a) illustrates the case in which two component terms have $\lambda_{33/34}$ values of 0.505 and 0.515, respectively, and involve fractionations having the same sign. In this case, the net fractionation will be relatively large (i.e., because the two components work in the same direction), and the net $\lambda_{33/34}$ value will be the weighted average of the two components. Panel (b) illustrates the case in which the two components have these same $\lambda_{33/34}$ values (0.505 and 0.515) but involve fractionations of opposite sign. In this case, the net fractionation is relatively small (because the smaller of the fractionations partially cancels the larger), but the net $\lambda_{33/34}$ value can take on values outside of the range defined by the two components.

Table 2
Vibrational frequencies of SF6 vapor.

Mode	Degeneracy	Measured frequency (cm^{-1})*
ν1	1	773.5
ν2	2	641.7
		641.7
ν3	3	947.5
		947.5
		947.5
ν4	3	615.5
		615.5
		615.5
ν5	3	525.0
		525.0
		525.0
ν6	3	347.0
		347.0
		347.0

* Taken from the JANAF data base; Chase et al. (1985).

Table 3
Measured phonon spectrum of SF6 ice.

Frequency (cm^{-1})	Inferred equivalent mode in vapor
23.4	Lattice
31.5	Lattice
42.5	Lattice
55.5	Lattice
61.2	Lattice
66	Lattice
77	Lattice
83.5	Lattice
776	ν1
777	ν1
639.3	ν2
641.5	ν2
645.3	ν2
646.4	ν2
897.2	ν3
900.5	ν3
902	ν3
915.6	ν3
916.5	ν3
1002	ν3
606.3	ν4
607.4	ν4
610.2	ν4
618	ν4
523.3	ν5
524.2	ν5
535	ν5

Salvi and Schettino (1979); including only bands assigned to fundamental modes, including lattice modes.

1974). In SF_6 ice, in particular, there are modes of vibration that are generally similar in frequency to ν_3 and ν_4 in vapor, and thus could be thought of as approximating intramolecular vibrations in the molecular ice, but are significantly lower in frequency than ν_3 and ν_4 in vapor (compare the measured ν_3 and ν_4 frequencies in Tables 2 and 3; increases in frequency of some other frequencies in ice is more subtle and has no influence on isotopic fractionation because the central S atom in SF_6 is stationary relative to the molecular center of mass for the ν_1, ν_2, ν_5 and ν_6 modes; Shurvell and Bernstein, 1969; Salvi and Schettino, 1979; McDowell and Krohn, 1986; Boudon et al., 2006). Thus, intramolecular bonds in SF_6 vapor have higher frequencies of vibration than broadly equivalent modes in ice for the modes that influence isotopic fractionation. This effect, considered in isolation, will promote concentration of heavy isotopes into vapor because the decrease in free energy associated with heavy isotope substitution scales with vibration frequency when all other factors are constant. That is, the zero point energy change (ΔZPE) under the harmonic oscillator approximation is:

$$\Delta ZPE \propto 1/2h\Delta v \propto 1/2hv(1-(\mu/\mu')^{1/2})$$

i.e., for a given reduced mass, higher frequency corresponds to higher change in frequency, and thus higher energy change, on isotopic substitution. Thus, spectroscopic data and simple physical reasoning suggest that intermolecular and intramolecular contributions to equilibrium S isotope fractionations between SF_6 ice and vapor are opposite in sign; i.e., we should expect that the net fractionation could take on a non-canonical mass law (as in Fig. 5b).

We attempted to evaluate this hypothesis further through statistical thermodynamic models based on the modeled vibrational properties of SF_6 vapor and ice and their dependences on isotopic compositions. The results of these models support some elements of our hypothesis—most importantly, the reversed vapor pressure isotope effect for SF_6 ice—but fails in two important (and perhaps related) respects: the predicted phonon spectrum of ice disagrees with that measured by Raman spectroscopy; and the amplitude of the predicted fractionation is about an order of magnitude larger than that observed in our experiments. We suspect these errors reflect uncertainties and simplifications in our models of the solid phonon spectrum (and possibly also simplifications in our treatment of vibrational isotope effects in the vapor). Regardless, these models do not usefully support or disprove our hypothesis, which depends upon a relatively subtle effect of nearly canceling isotope effects on intra- and inter-molecular vibrations (i.e., any model that strongly miss-calculates the relative sizes of these two terms should fail to reveal the resulting exotic mass law we predict). Nevertheless, our efforts may serve as a starting point for more sophisticated and complete models of this and related systems; so we present this work in the Supplementary Information file.

4.2. Experimental artifacts?

Despite the evidence that many of our experiments closely approached or achieved equilibrium, we also consider several potential experimental and analytical artifacts that might compromise our interpretations. First, it is important to note that our experiments involved exchange of condensate in a cold trap with a vapor reservoir interconnected with a room-temperature reservoir. Thus, the vapor is exposed to a temperature gradient, so it is possible that there is isotopic fractionation due to thermal diffusion (i.e., a

fractionation whereby heavy isotopologues gravitate toward a cold region and light isotopologues toward a hot region in a temperature gradient; Gibbs, 1928). Such effects form the basis of the ^{15}N paleothermometer in N_2 trapped in glacial ice (Severinghaus et al., 1998) and have been studied in the laboratory (Grachev and Severinghaus, 2003). A recent study of gas-phase fractionations of O_2 and SF_6 in a temperature gradient found non-canonical mass laws (Sun and Bao, 2011a,b), though the fractionations they observed appear to have been time-varying, possibly non-equilibrium effects. We estimate the Rayleigh number of the gas phase under the conditions of our experiments is on the order of 10^2–10^3, a transitional regime in which it is unclear whether vapor convection will erase compositional gradients. It is imaginable that our observations reflect the combined influences of a large reversed vapor pressure isotope effect having a canonical mass law and a thermal diffusion fractionation that is opposite in sign (i.e., heavy isotopes go into the cold trap) and somewhat lower slope. Such a combined fractionation might resemble, at least topologically, the argument presented in Fig. 5.

However, it can be shown relatively easily that this scenario is implausible because it requires a large (several per mil) thermal diffusion fractionation, inconsistent with our demonstration in Experiment 2 that thermal diffusion is negligible in our apparatus (at least over the pressures and time scales of our experiments). For example, the measured net ice–vapor fractionation observed in our experiments could be produced if the thermal diffusion fractionation had a magnitude equal to the Knudsen diffusion fractionation for SF_6 vapor and a mass law following the kinetic theory of gases: $\alpha_{33} = 1.00342$, $\alpha_{34} = 1.00683$ and $\lambda = 0.5017$ (where α is the isotope ratio of the cold end divided by the isotope ratio of the hot end of the temperature gradient). If this were combined with a vapor pressure isotope effect having $\alpha_{33} = 0.9952$, $\alpha_{34} = 0.9907$, and $\lambda = 0.515$, the net fractionation ($\alpha_{net} = \alpha_{VPIE} \times \alpha_{thermal\ diffusion}$) would be consistent with our experimental observations at 155 K. However, we observe a negligibly small fractionation ($\alpha_{34} \leqslant 1.0001$) when vapor is exposed to an 80 K temperature gradient in the absence of condensed SF_6 (Experiment 2, Table 1). It is implausible that the thermal diffusion fractionation could go from negligible to quite large with such a modest proportional increase in temperature gradient. Similarly, it is not possible to match our experimental observations by combining any vapor pressure isotope effect having a canonical mass law with a thermal diffusion fractionation equal to that we measured in Experiment 2.

A more general alternative interpretation of our results is that the net fractionations we observed were actually the combination of two or more fractionations that might have differed in sign and/or mass law, such that their combined effect mimicked a single fractionation having a non-canonical mass law (again, in a way topologically resembling Fig. 5 but consisting of two or more separate fractionation mechanisms rather than two or more vibrational modes of a single equilibrium fractionation). This is a reasonable interpretation of several recent experiments that found non-canonical mass laws for fractionations exhibited by the products of complex, multi-stage (and apparently kinetically controlled) reactions (Miller et al., 2002; Watanabe et al., 2009; Oduro et al., 2011). However, all of the data for ice–vapor and sorbate–vapor fractionations in Fig. 4 conform to a single slope (i.e., they are consistent with a single mass exponent)—even for experiments that failed to exhibit the full equilibrium (i.e., reversible) fractionation, either because the experiment was too short in duration or had too small of a fraction of SF_6 as ice. Only under fortuitous circumstances would two or more fractionations that differ in mass law combine to create a constant mass law across a significant range of net fractionations (i.e., just the right balance of relative and absolute amounts of each reaction). Perhaps this cannot be disproven, but it strikes us an implausible explanation.

4.3. Alternate causes of non-canonical VPIE's

A variety of physical mechanisms have been proposed to explain non-canonical (including mass-independent) fractionations. We conclude our discussion by considering whether any other than the one we have proposed could be causes of the non-canonical fractionation we observe for the ice–vapor and sorbate–vapor vapor pressure isotope effects of SF_6.

Perhaps the best studied non-canonical mass laws for isotopic fractionations involve photolysis or other photochemical reactions (Weston, 2006 and references therein). However, our experimental setup lacked any light source in the frequency range capable of photolysis of SF_6 or production of photochemical reactants (e.g., O^{1D}). Furthermore, the time independence, reversibility, and mass balance of our experiments indicate we did not observe the effects of a fractionating loss of sulfur to a photochemical (or other) sink.

Nuclear volume effects can exhibit a range of mass exponents that include non-canonical mass laws (Bigeleisen, 1996). However, these effects are generally only significant for the very heavy elements (e.g., U). A recent evaluation of such effects for sulfur predicts them be on the order of 0.02‰ per AMU or smaller (Schauble, 2007)—2 orders of magnitude smaller than the fractionations observed in our experiments.

Nuclear spin effects, or coupling between nuclear and electron spin (also sometimes referred to as 'magnetic isotope effects'), can potentially lead to non-canonical fractionations when one of the isotopes involved has an odd mass number (i.e., ^{33}S; Turro, 1983). These effects generally are expected in chemical systems in which the radical pair mechanism is involved in an irreversible, photo-chemically excited reaction (e.g., Oduro et al., 2011). SF_6 is a closed-shell species (i.e., it has no unpaired electrons), so it is difficult to imagine how nuclear spin effects could have contributed to the fractionations we observe. It is worth noting that SF_6 is unusual in that it has a 'hypervalent' or 'hypercoordinated' electronic structure, consisting of three three-center-4-electron ('3c-4e') bonds (Musher, 1969). Given the limited amount of work that has been done on magnetic isotope effects, it is worth considering whether such unusual electronic structures could permit magnetic isotope effects even in closed-shell species. Never-

theless, because the sulfur bonding environments in condensate and vapor phases in our experiments are similar (i.e., all are SF_6), it is difficult to imagine how a magnetic isotope effect, even if it existed in some heterogeneous reactions involving decomposition of SF_6, could have driven the vapor pressure isotope effects we observe.

Lasaga et al. (2008) suggest that isotope effects on vibrational frequencies of weak bonds can, under certain circumstances, create a mass filter in which bound and unbound populations exhibit non-canonical (even mass-independent) isotopic fractionations with respect to one another. If correct, this theory provides a quantum–mechanical mechanism, beyond that contained in the Urey–Bigeleisen quantum mechanical theory, by which thermodynamically controlled isotope exchange equilibria could mimic the non-canonical mass laws that are conventionally interpreted as photochemical in origin. More recently, Balan et al. (2009) argue that this model makes a truncation error that is responsible for the predicted non-canonical effects and that no such effects are actually expected to accompany sorption.

The chemical physics of the mechanism we invoke to explain the experimental data presented here might appear, superficially, analogous to that presented in Lasaga et al. (2008). However, there is an important distinction between these hypotheses: Lasaga et al. (2008) suggested that the physics of a quantum oscillator can lead to non-canonical behavior under specific conditions—even for the simplest case of a point mass undergoing a single mode of harmonic oscillation. We instead suggest that even when the physics of an oscillator is well described by standard theory, the combination of two or more modes of vibration—each of which, in isolation, would follow canonical mass dependence—can produce a non-canonical mass law for the net fractionation.

In any event, there are several inconsistencies between our results and the Lasaga et al. (2008) hypothesis. First, that hypothesis does not predict the existence of vapor pressure isotope effects that are 'reversed' (i.e., where the ratio of heavy to light isotopes in the vapor is higher than that in the condensed phase), as we observe. Second, the effect Lasaga describes should only operate at elevated temperatures (~500 K), where a significant proportion of the population of adsorbed molecules is in a high vibrational quantum state. At the temperatures of our ice–vapor and adsorbate–vapor experiments (137–188 K), essentially all intermolecular bonds should be in low-quantum number vibrational states. For example, given a condensate bond energy of 0.25 eV, (broadly within the range of intermolecular bonds in molecular ices and consistent with the latent heat of sublimation of SF_6 ice; Ohta et al., 1994) and an assumed temperature of 150 K, one expects 20 bound vibrational states, in which 98.7% of all bonds will be in the $N = 0$, 1, or 2 states and 0.00058% of bonds will be in the $N = 10$–19 states (calculated using the model of Balan et al., 2009). We observe no significant variation in mass exponent between 137 and 188 K, whereas the Lasaga hypothesis predicts that the mass exponent should be temperature-dependent in the temperature range where mass-law anomalies first appear. Finally, we find no evidence for the existence of the exceptional non-canonical exponents ($\lambda_{33/34}$ equal to −1 or 1) predicted by Lasaga et al. (2008) for some systems.

4.4. Broader implications and conclusions

Recent discussion regarding the definition and meaning of mass-dependent and mass-independent isotopic fractionations has been largely framed by the predicted mass laws for relatively simple chemical and physical fractionation mechanisms, such as the vibrational energy of the harmonic oscillator and the kinetic theory of gases (Young et al., 2002; Otake et al., 2008). Our results present a challenge to this paradigm; i.e., idealized or simplified forms of these theories are inadequate for understanding our experimental results, even though the case we have examined is a relatively straightforward thermodynamic phenomenon (the vapor pressure isotope effect of a small, symmetric molecule).

The chemical physics literature provides precedence for our results and hypothesized explanation. Non-canonical mass laws have been observed in hydrogen isotope exchange equilibria (i.e., non-canonical $\lambda_{T/D}$ values) among H_2, hydrogen halides, and methane, and more subtle but similar non-canonical fractionations of $^{14}C/^{13}C/^{12}C$ ratios have been observed in the vapor pressure isotope effect of liquid methane (Jansco and Van Hook, 1974, and references therein). It has been argued that non-canonical mass laws in these systems arise when fractionations undergo a temperature-dependent 'crossover' (i.e., the fractionation has one sign at high temperature and a different sign at lower temperature; e.g., Stern and Vogel, 1971; Weston, 1973; Skaron and Wolfsberg, 1980; Kotaka et al., 1992; Horita and Wesolowski, 1994; Deines, 2003). A non-canonical fractionation in such systems can arise because the crossover temperature for one isotope ratio (e.g., D/H) differs from that for another isotope ratio (e.g., T/H), causing the slope in a α_D vs. α_T diagram to rotate sharply as the fractionations pass through 0.

In the narrowest descriptions of this phenomenon (e.g., Deines, 2003), non-canonical mass laws occur only over a narrow range in temperature (approximately a few degrees) on either side of the crossover temperatures (i.e., the temperatures at which the sign of the fractionation changes) and vary strongly in mass exponent with temperature. However, these non-canonical mass laws can also occur in systems that lack a crossover. Kotaka et al. (1992) demonstrate that any exchange equilibrium involving large variations in reduced mass can exhibit a non-canonical mass exponent. For example, for H_2 – HX exchange equilibria (where X is a halogen), non-canonical mass laws occur because the proportional change in reduced mass for H/D vs. H/T exchange differs between molecular hydrogen and hydrogen-halides; as a result, D/H fractionations exhibit markedly different temperature dependences than T/H fractionations, and at moderate temperature (typically 200–500 K), non-canonical effects can be observed, even when there is no nearby temperature-dependent crossover. The vapor pressure isotope effects of H_2 and CH_4 also exhibit non-canonical mass laws that arise because

rotational–vibrational coupling in the liquid (Bigeleisen et al., 1967) leads to a dependence of the heat of vaporization on molecular moments of inertia (which differ between heteronuclear species, like HD, HT and DT, and homonuclear species, like H_2, D_2 and T_2). Finally, it is recognized that molecular polarizabilities can change on isotopic substitution, leading to an isotopic dependence of the force constants of intermolecular bonds (Wolfsberg, 1963; Grootes et al., 1969). This factor also has potential to lead to non-canonical mass laws; in fact, it is possible that this phenomenon contributes to the mass law we observe for the SF_6 vapor pressure isotope effect.

The collective weight of these past studies and our present study suggest there is significant potential for non-canonical mass laws for isotopic fractionations during 'conventional' chemical reactions (i.e., thermodynamic equilibria and irreversible reactions in which fractionations are driven by vibrational isotope effects). An open question is whether non-canonical mass laws of this kind occur in nature and impact geochemical records (e.g., the ^{17}O anomalies of atmospheric O_2 or H_2O or the ^{33}S anomalies of sulfides and sulfates). We suggest several guidelines for searching for such examples. First, we suspect that non-canonical mass laws analogous to the SF_6 vapor pressure isotope effect will generally involve low-amplitude overall isotope fractionations (i.e., a few per mil difference in $\delta^{18}O$ or $\delta^{34}S$ between reactants and products). This is because the greatest opportunity for non-canonical mass laws will arise when two or more vibrational isotope effects that influence the same reaction have opposite sign and partially cancel one another. However, we note that the H/D/T isotopologues of water exhibit large variations in the mass law of their vapor pressure isotope effect when the D/H ratio fractionation is tens of per mil. Systems that exhibit temperature-dependent crossovers (e.g., the oxygen isotope fractionations between water and magnetite, hematite, goethite, and albite; e.g., Yapp, 1990) are obvious places to look, as are reactions that exhibit peculiar temperature dependencies—another indicator that the net observed fractionation reflects the balance of two or more competing vibrational terms. In addition, there are classes of fractionations that are not well explored by previous experiments but that might be expected to exhibit non-canonical behaviors based on the molecular structures of participating species. Instances in which reactions occur without breaking the bonds between the isotopic species of interest and its immediate neighbors are particularly attractive, because the effect of isotopic mass on reaction rate or equilibrium constant will be indirect (i.e., a sort of secondary isotope effect) and could involve several modes of molecular vibration that differ from one another in reduced mass. Enzymatic reactions may be particularly attractive targets because of the large sizes and complex vibrational energetics of reactive sites. Other attractive targets include fractionations involving dissolution or outgassing of volatile gases (e.g., dimethyl sulfide and its relatives) from seawater (i.e., solvation/desolvation of species in which sulfur is shielded from surrounding water molecules). While it is possible that non-canonical mass laws of this kind exist for elements other than O and S (e.g., Si, Ca, Fe, etc.), isotopic fractionations in these systems are small, and it would be challenging to observe the mass laws with sufficient precision to recognize a non-canonical mass law.

ACKNOWLEDGMENTS

Edwin Schauble contributed significantly to the model presented in the Supplementary information file, including both helpful leading questions following an early presentation of our experimental results and guidance regarding the calculations we present—any remaining errors are trivial compared to the ones he repaired! Albert Jambon is thanked for sharing a cryogenic trap used during the completion of this study. This work was initiated during a sabbatical JME spent in the IPGP laboratories for stable isotope geochemistry; he thanks the IPGP foreign visitor program and the members of that laboratory for their help and collegial discussions during this stay. This paper was improved in response to reviews by Gerardo Dominguez, James Farquhar and two anonymous reviewers.

APPENDIX A. SUPPLEMENTARY DATA

Supplementary data associated with this article can be found, in the online version, at http://dx.doi.org/10.1016/j.gca.2012.12.048.

REFERENCES

Balan E., Cartigny P., Blanchard M., Cabaret D., Lazzeri M. and Mauri F. (2009) Theoretical investigations of the anomalous equilibrium fractionation of multiple sulfur isotopes during adsorption. *Earth Planet. Sci. Lett.* **284**, 88–93.

Bigeleisen J. (1996) Nuclear size and shape effects in chemical reactions. Isotope chemistry of the heavy elements. *J. Am. Chem. Soc.* **118**, 3676–3680.

Bigeleisen J. and Mayer M. G. (1947) Calculation of equilibrium constants for isotopic exchange reactions. *J. Chem. Phys.* **15**, 261–267.

Bigeleisen J. and Wolfsberg M. (1958) Theoretical and experimental aspects of isotope effects in chemical kinetics. *Adv. Chem. Phys.* **1**, 15–76.

Bigeleisen J., Cragg C. B. and Jeevanan M. (1967) Vapor pressures of isotopic methanes – evidence for hindered rotation. *J. Chem. Phys.* **47**, 4335–4346.

Boudon V., Domenech J. L., Ramos A., Bermejo D. and Willner H. (2006) High-resolution stimulated Raman spectroscopy and analysis of the n_2, n_5 and $2n_6$ bands of $^{34}SF_6$. *Mol. Phys.* **104**, 2653–2661.

Chacko T., Cole D. R. and Horita J. (2001) Equilibrium oxygen, hydrogen and carbon isotope fractionation factors applicable to geologic systems. In *Stable Isotope Geochemistry, Reviews in Mineralogy*, vol. 43 (eds. J. W. Valley and D. Cole). pp. 1–81.

Chase, Jr., M. W., Davies C. A., Downey, Jr., J. R., Frurip D. J., McDonald R. A. and Syverud A. N. (1985) JANAF thermochemical tables (3rd ed.). *J. Phys. Chem. Ref. Data* **14**(Suppl. 1), 1.

Clayton R. N. (2002) Solar System – self-shielding in the solar nebula. *Nature* **415**, 860–861.

Deines P. (2003) A note on intra-elemental isotope effects and the interpretation of non-mass-dependent isotope variations. *Chem. Geol.* **199**, 179–182.

Eiler J. M., Kitchen N. and Rahn T. A. (2000) Experimental constraints on the stable-isotope systematics of CO_2 ice/vapor

systems and relevance to the study of Mars. *Geochim. Cosmochim. Acta* **64**, 733–746.

Farquhar J. and Wing B. A. (2003) Multiple sulfur isotopes and the evolution of the atmosphere. *Earth Planet. Sci. Lett.* **213**, 1–13.

Firanescu G, Luckhaus D and Signorell R (2008) Phase, shape and architecture of SF_6 and SF_6/CO_2 aerosol particles: infrared spectra and modeling of vibrational excitons. *J. Chem. Phys.* **128**, article no. 184301.

Gibbs J. W. (1928) Collected Works.

Grachev A. M. and Severinghaus J. P. (2003) Laboratory determination of thermal diffusion constants for $^{29}N_2/^{28}N_2$ in air at temperatures from −60 to 0 °C for reconstruction of magnitudes of abrupt climate changes using the ice core fossil-air paleothermometer. *Geochim. Cosmochim. Acta* **67**, 345–360.

Grootes P. M., Mook W. G. and Vogel J. C. (1969) Isotopic fractionation between gaseous and condensed carbon dioxide. *Z. Phys.* **221**, 257–273.

Horita J. and Wesolowski D. J. (1994) Liquid–vapor fractionation of oxygen and hydrogen isotopes of water from the freezing to the critical temperature. *Geochim. Cosmochim. Acta* **58**, 3425–3437.

Hulston J. R. and Thode H. G. (1965) Variations in ^{33}S, ^{34}S and ^{36}S contents of meteorites and their relations to chemical and nuclear effects. *J. Geophys. Res.* **70**, 3475–3484.

Hurly J. J., Defibaugh D. R. and Moldover M. R. (2000) Thermodynamic properties of sulfur hexafluoride. *Int. J. Thermophys.* **21**, 739–765.

Jansco G. and Van Hook W. A. (1974) Condensed phase isotope effects (Especially vapor pressure isotope effects). *Chem. Rev.* **74**, 689–750.

Kotaka M., Okamoto M. and Bigeleisen J. (1992) Anomalous mass effects in isotopic exchange equilibria. *J. Am. Chem. Soc.* **114**, 6436–6445.

Lasaga A. C., Otake T., Watanabe Y. and Ohmoto H. (2008) Anomalous fractionation of sulfur isotopes during heterogeneous reactions. *Earth Planet. Sci. Lett.* **268**, 225–238.

Luz B., Barkan E., Yam R. and Shemesh A. (2009) Fractionation of oxygen and hydrogen isotopes in evaporating water. *Geochim. Cosmochim. Acta* **73**, 6697–6703.

McDowell R. S. and Krohn B. J. (1986) Vibrational levels and anharmonicity in SF_6 — II. Anharmonic and potential constants. *Spectrochim. Acta* **42A**, 371–385.

Miller M. F., Franchi I. A., Thiemens M. H., Jackson T. L., Brack A., Kurat G. and Pillinger C. T. (2002) Mass-independent fractionation of oxygen isotopes during thermal decomposition of carbonates. *Proc. Natl. Acad. Sci. USA* **99**, 10,988–10,993.

Musher J. I. (1969) The chemistry of hypervalent molecules. *Angew. Chem. Int.* **8**, 54–68.

Oduro H., Harms B., Sintimc H. O., Kaufman A. J., Cody G. and Farquhar Jame (2011) Evidence of magnetic isotope effects during thermochemical sulfate reduction. *Proc. Natl. Acad. Sci. USA* **108**, 17635–17638.

Ohta T., Yamamuro O. and Suga H. (1994) Heat capacity and enthalpy of sublimation of sulfur-hexafluoride. *J. Chem. Thermodyn.* **26**, 319–331.

Ono S., Wing B., Johnston D., Farquhar J. and Rumble D. (2006) Mass-dependent fractionation of quadruple stable sulfur isotope system as a new tracer of sulfur biogeochemical cycles. *Geochim. Cosmochim. Acta* **70**, 2238–2252.

Otake T., Lasaga A. C. and Ohmoto H. (2008) Ab initio calculations for equilibrium fractionations in multiple sulfur isotope systems. *Chem. Geol.* **249**, 357–376.

Rahn T. and Eiler J. M. (2001) Experimental constraints on the fractionation of $^{13}C/^{12}C$ and $^{18}O/^{16}O$ ratios due to adsorption of CO_2 on mineral substrates at conditions relevant to the surface of Mars. *Geochim. Cosmochim. Acta* **65**, 839–846.

Robert F., Rejoumichel A. and Javoy M. (1992) Oxygen isotopic homogeneity of the earth – New evidence. *Earth Planet. Sci. Lett.* **108**, 1–9.

Salvi P. R. and Schettino V. (1979) Infrared and Raman spectra and phase transition of the SF_6 crystal. Anharmonic interactions and two-phonon infrared absorption. *Chem. Phys.* **40**, 413–424.

Schauble E. (2007) Role of nuclear volume in driving equilibrium stable isotope fractionation of mercury, thallium, and other very heavy elements. *Geochim. Cosmochim. Acta* **71**, 2170–2189.

Severinghaus J. P., Sowers T., Brook E. J., Alley R. B. and Bender M. L. (1998) Timing of abrupt climate change at the end of the Younger Dryas interval from thermally fractionated gases in polar ice. *Nature* **391**, 141–146.

Shurvell H. F. and Bernstein H. J. (1969) Raman spectrum of solid sulfur hexafluoride. *J. Mol. Spectrosc.* **30**, 153–157.

Skaron S. and Wolfsberg M. (1980) Anomalies in the fractionation by chemical equilibrium of $^{18}O/^{16}O$ relative to $^{17}O/^{16}O$. *J. Chem. Phys.* **72**, 6810–6811.

Stern M. J. and Vogel P. C. (1971) Relative tritium–deuterium isotope effects in absence of large tunneling factors. *J. Am. Chem. Soc.* **93**, 4664–4675.

Sun T. and Bao H. (2011a) Non-mass-dependent ^{17}O anomalies generated by a superimposed thermal gradient on a rarefied O_2 gas in a closed system. *Rapid Commun. Mass Spectrom.* **25**, 20–24.

Sun T. and Bao H. (2011b) Thermal-gradient induced non-mass-dependent isotope fractionation. *Rapid Commun. Mass Spectrom.* **25**, 765–773.

Thiemens M. H. and Heidenreich J. E. (1983) The mass-independent fractionation of oxygen – a novel isotope effect and its possible cosmochemical implications. *Science* **219**, 1073–1075.

Thornton S. T. and Rex A. (1993) *Modern Physics for Scientists and Engineers*. Saunders College Publishing.

Turro N. J. (1983) Influence of nuclear spin on chemical reactions: magnetic isotope and magnetic field effects (A Review). *Proc. Natl. Acad. Sci. USA* **80**, 609–621.

Van Hook W. A. (1968) Vapor pressures of the isotopic waters and ices. *J. Phys. Chem.* **72**, 1234–1244.

Watanabe Y., Farquhar J. and Ohmoto H. (2009) Anomalous fractionations of sulfur isotopes during thermochemical sulfate reduction. *Science* **324**, 370–373.

Weston, Jr, R. E. (1973) Relation between D-H and T-H isotopic fractionation in some reactions of chemical interest. *Z. Naturforsch. [A]* **28**, 177–184.

Weston, Jr, R. E. (2006) When is an isotope effect non-mass dependent? *J. Nucl. Sci. Technol.* **43**, 295–299.

Wolfsberg M. (1963) Isotope effects on intermolecular interactions and isotopic vapor pressure differences. *J. Chim. Phys. Phys. – Chim. Biol.* **60**, 15–22.

Yapp C. J. (1990) Oxygen isotopes in iron (III) oxides. 1. Mineral-water fractionation factors. *Chem. Geol.* **85**, 329–335.

Young E. D., Galy A. and Nagahara H. (2002) Kinetic and equilibrium mass-dependent isotope fractionation laws in nature and their geochemical and cosmochemical significance. *Geochim. Cosmochim. Acta* **66**, 1095–1104.

Associate editor: Edwin Schauble